



Published in final edited form as:

J Biomol Screen. 2016 December ; 21(10): 1090–1099. doi:10.1177/1087057116675315.

Development of an *in vitro* model to screen CYP1B1-targeted anticancer prodrugs

Zhiying Wang, Yao Chen, Laura M. Drbohlav, Judy Qiju Wu, Michael Zhuo Wang

Department of Pharmaceutical Chemistry (ZW, YC, LMD and MZW) and Department of Medicinal Chemistry (JQW), School of Pharmacy, The University of Kansas, 2095 Constant Avenue, Lawrence, KS, USA

Abstract

Cytochrome P450 1B1 (CYP1B1) is an anticancer therapeutic target due to its overexpression in a number of steroid hormone-related cancers. One anticancer drug discovery strategy is to develop prodrugs specifically activated by CYP1B1 in malignant tissues to cytotoxic metabolites. Here, we aimed to develop an *in vitro* screening model for CYP1B1-targeted anticancer prodrugs using the KLE human endometrial carcinoma cell line. KLE cells demonstrated superior stability of *CYP1B1* expression relative to transiently transfected cells and did not express any appreciable amount of cognate CYP1A1 or CYP1A2, which would have compromised the specificity of the screening assay. The effect of two CYP1B1-targeted probe prodrugs on KLE cells was evaluated in the absence and presence of a CYP1B1 inhibitor to chemically “knockout” CYP1B1 activity (CYP1B1-inhibited). Both probe prodrugs were more toxic to KLE cells than to CYP1B1-inhibited KLE cells and significantly induced G0/G1 arrest and decreased S phase in KLE cells. They also exhibited pro-apoptotic effects in KLE cells, which were attenuated in CYP1B1-inhibited KLE cells. In summary, a KLE cell-based model has been characterized to be suitable for identifying CYP1B1-targeted anticancer prodrugs and should be further developed and employed for screening chemical libraries.

Keywords

CYP1B1; prodrug; targeted anticancer; drug screening; endometrial cancer

INTRODUCTION

Cytochrome P450 1B1 (CYP1B1) belongs to a superfamily of heme-containing enzymes, cytochrome P450s, which play a central role in the oxidative metabolism of xenobiotics and endogenous compounds.¹ In particular, this enzyme catalyzes the metabolic activation of procarcinogens, such as the polycyclic aromatic hydrocarbons² benzo(*a*)pyrene and 7,12-dimethylbenz[*a*]anthracene and the estrogenic 17 β -estradiol (E2).³ CYP1B1 is overexpressed in multiple human cancers, including breast,⁴ colon,⁵ prostate,⁶ endometrium⁷ and ovary.⁸ Recently, multiple molecular epidemiological studies have

corroborated an association between *CYP1B1* genetic polymorphisms and cancer risk, especially for steroid hormone-related cancers (*i.e.*, prostate, breast, ovarian and uterine/endometrial cancers),^{9–11} where particularly high *CYP1B1* expression levels have been observed.¹² Importantly, the enzyme either is absent or expressed at low levels in corresponding normal tissues, making it an attractive target for anticancer therapeutics and chemoprevention.^{13, 14}

CYP1B1 and two other enzymes, *CYP1A1* and *CYP1A2*, constitute the *CYP1* family. Nearly 40% amino acid sequence identity is shared between them. *CYP1B1* and *CYP1A1* are predominantly expressed in extrahepatic tissues, whereas *CYP1A2* mainly is found in the liver. These *CYP1* enzymes have distinct substrate specificities, but do overlap in some cases.¹ For example, both *CYP1B1* and *CYP1A1* catalyze the hydroxylation of E2. However, *CYP1B1* preferentially hydroxylates the C-4 position to form 4E2,³ whereas *CYP1A1* mainly hydroxylates the C-2 position to form 2E2.¹⁵ Since 4E2 has been shown to be carcinogenic in animal models¹⁶ and in human breast¹⁷ and myometrium,¹⁸ *CYP1B1* is believed to play an important role in carcinogenesis by activating E2 to 4E2. Furthermore, *CYP1B1* also has been shown to contribute to carcinogenesis by activating polycyclic aromatic hydrocarbons to mutagens^{2, 14} and to play a significant role in promoting cancer cell proliferation, progression and migration in head and neck and endometrial cancers.^{7, 19} However, the development of selective inhibitors for *CYP1B1* has been hampered by overlap with *CYP1A1* and/or *CYP1A2*.

An alternative, perhaps more ideal approach for *CYP1B1*-targeted anticancer strategies is to develop prodrugs specifically activated by *CYP1B1* in malignant tissues to cytotoxic metabolites. DMU-135 represents the first such prodrug, designed to be activated by *CYP1B1* within tumors to a tyrosine kinase inhibitor.²⁰ In addition, resveratrol, a natural product found in red wine, is hydroxylated by *CYP1B1* to form piceatannol, which has known anticancer properties.²¹ Recently, rationally designed prodrugs have also been shown to be bioactivated by *CYP1B1*, although cytotoxic metabolites were also generated by *CYP1A1* and *CYP3A4*.²² The discovery of new *CYP1B1*-activated prodrugs has been hindered by the lack of a relevant drug discovery model to enable screening of large chemical libraries. The human uterus adenocarcinoma cell line KLE, derived from a poorly differentiated endometrial cancer with a defective estrogen receptor, possesses tumorigenic activity in nude mice.²³ Relative *CYP1B1* expression in several human endometrial cancer cell lines, including KLE, Ishikawa, HEC-1-B and RL95–2, has been investigated using real-time PCR; KLE cells had the highest expression.⁷ Hence, the human KLE endometrial cancer cell line was selected, in this study, to develop a screening model for *CYP1B1*-targeted anticancer prodrugs.

To demonstrate the validity of the KLE cell-based screening model, two antiparasitic prodrugs, DB289 and DB844, were employed (Supplemental Figure 1). *CYP1B1* previously was shown to biotransform DB289 to its primary metabolite M1.²⁴ In addition, *CYP1B1* and *CYP1A1*, but not *CYP1A2*, were found to catalyze the oxidative metabolism of DB844 to an oxaziridine intermediate and subsequently release nitric oxide *via* intramolecular rearrangement of the adjacent O-methyl group.²⁵ Hence, we hypothesized that DB289 and DB844 may serve as probe prodrugs that are activated by *CYP1B1* to form more cytotoxic

metabolites. As such, we examined the cytotoxic, cell cycle, and pro-apoptotic effects of DB289 and DB844 on KLE cells in the absence and presence of a potent CYP1B1 inhibitor. These results support the use of KLE cell-based screening assays to discover new CYP1B1-targeted anticancer prodrugs.

MATERIALS AND METHODS

Chemicals and reagents

DB289 (2,5-bis[4-amidinophenyl]furan-bis-*O*-methylamidoxime) and DB844 (N-methoxy-6-[5-[4-(N-methoxyamidino)phenyl]-furan-2-yl]-nicotinamidine) were kindly provided by the Consortium for Parasitic Drug Development (CPDD; The University of North Carolina at Chapel Hill, Chapel Hill, NC). Resazurin sodium salt, α -naphthoflavone (α -NF), 7-ethyl-resorufin (7-ER), resorufin, Triton X-100, DMSO, ammonium bicarbonate, dithiothreitol, iodoacetamide and D-glucose were purchased from Sigma-Aldrich Co. (St. Louis, MO). Methyl tert-butyl ether (MTBE; HPLC-grade) was purchased from Fisher Scientific (Pittsburg, PA). E2, 2E2 and 4E2 standards were purchased from Steraloids Inc. (Newport, RI). Dulbecco's modified Eagle's medium (DMEM), DMEM/F-12 (1:1), Williams's E medium (WME), TrypLE™ Express, fetal bovine serum (FBS), GlutaMax™, Lipofectamine® 2000 and TRIzol® reagent were purchased from Life Technologies (Carlsbad, CA). High Capacity cDNA Reverse Transcription kits were purchased from Applied Biosystems (Foster City, CA). Human CYP1B1 plasmid DNA (CYP1B1-pCMV6-Entry) and pCMV10 empty vector were purchased from OriGene Technologies, Inc. (Rockville, MD). A Light Cycler 480 SYBR Green I master kit was purchased from Roche Applied Science (Foster City, CA). MVP human liver total RNA (catalog # 540017; A260/A280 1.8; pool of 3 donors, male and female, ages 30, 44 and 55) was purchased from Agilent Technologies (Santa Clara, CA). A BCA protein assay kit was purchased from Pierce Biotechnology (Rockford, IL). A BioRad protein estimation kit was purchased from BioRad (Hercules, CA). BD Pharmingen™ PI/RNase staining buffer and Annexin V-FITC Apoptosis Detection Kit I were purchased from BD Biosciences (San Jose, CA).

Cell culture

KLE and HEK293T (human embryonic kidney cell line) cells were purchased from American Type Culture Collection (Manassas, VA). HepaRG™ (human hepatoma cell line) cells and additives for HepaRG Growth and Differentiation mediums were purchased from Biopredic International (Overland Park, KS). KLE and HEK293T cells were cultured in DMEM/F-12 (1:1) medium and DMEM, respectively, supplemented with 10% (v/v) FBS. HepaRG cells were cultured in Growth medium (WME supplemented with GlutaMax and HepaRG Growth Medium Supplement) for 2 weeks, followed by another 2 weeks in Differentiation medium (WME supplemented with GlutaMax and HepaRG Differentiation Medium Supplement). All cell lines were maintained at 37°C in 5% CO₂ and 95% humidity. Medium was refreshed twice a week for KLE cells and once every other day for HEK293T and HepaRG cells. Cells were harvested and passaged at 70% – 80% confluence using TrypLE™ Express. α -NF, a potent CYP1B1 inhibitor, was added to culture medium to “knock out” CYP1B1 catalytic activity in KLE cells, creating CYP1B1-inhibited KLE cells.

Transient transfection in HEK293T cells

The transfection of HEK293T cells was performed with Lipofectamine 2000. Briefly, 10 µg CYP1B1 plasmid DNA (or pCMV10 empty vector) and 25 µl Lipofectamine 2000 were added to separate tubes, each containing 500 µl serum-, antibiotic- and phenol red-free DMEM and incubated at room temperature for 5 min. The DNA and lipofectamine-containing DMEM then were mixed into one tube and incubated for an additional 20 min. The mixture (1 ml) was added to a 10-cm dish of HEK293T cells at 70–80% confluence to initiate transfection (time zero post-transfection). After a 6 h incubation at 37°C/5% CO₂, the medium was replaced with fresh culture medium and changed every other day thereafter.

Reverse transcription and real-time PCR

Total RNA was isolated from KLE, differentiated HepaRG and HEK293T cells in 12-well tissue culture plates using TRIzol reagent according to the manufacturer's protocol. The concentration and purity of RNA were determined using a Nanodrop[®] ND1000 spectrophotometer (Nanodrop Technologies, Wilmington, DE). One µg RNA then was reverse transcribed to cDNA using a High Capacity cDNA Reverse Transcription kit. After the first strand cDNA synthesis, 50 ng cDNA was amplified by real-time PCR using the LightCycler 480 SYBR Green I Master mix on an Applied Biosystems 7500 Fast real-time PCR system to evaluate *CYP1B1*, *CYP1A1* and *CYP1A2* expression. The primer sequences used in this study were: 5'-CTGTCTTGGGCTACCACATT -3' (forward) and 5'-GGATCAAAGTTCTCCGGGTTAG -3' (reverse) for *CYP1B1*; 5'-GTTCTACAGCTTCATGCAGAAGATG-3' (forward) and 5'-TTGGCGTTCTCATCCAGCT-3' (reverse) for *CYP1A1*; 5'-CTGTGGTTCCTGCAGAAAACAG-3' (forward) and 5'-CCCTTCTTGCTGTGCTTGAAC-3' (reverse) for *CYP1A2*. The mixture was amplified using the following conditions: 95°C for 10 min, then 40 cycles of 95°C for 10 s and 60°C for 35 s. Target gene expression was normalized to β-actin expression in each sample. The comparative threshold method was used to calculate the relative amount of mRNA in comparison to other samples.

Ethoxyresorufin-O-deethylase (EROD) activity assay

Cells were incubated with DMEM/F12 culture medium (FBS- and phenol red-free) containing 0.8 µM 7-ER at 37°C and 5% CO₂ for 1 h. After the incubation, culture plates were read on an Infinite[®] 200 PRO multimode reader (TECAN US, Inc., Morrisville, NC) to determine fluorescence intensity at 565 nm (excitation) and 595 nm (emission). The total cellular protein amount was used to normalize EROD activity.

E2 hydroxylation assay

KLE cells (day 11 post-seeding; grown in phenol red-free DMEM/F12 culture medium containing 10% FBS on a 10-cm cell culture dish) were incubated with E2 (10 µM in the complete culture medium; 2.0 mL) at 37°C and 5% CO₂ for 0, 20 and 60 min. At the end of incubation, cells and medium were mixed with MTBE (10 mL) to extract E2 hydroxylation metabolites and samples were reconstituted with isopropanol:water (1:1 v/v; 200 µL) prior to high pressure liquid chromatography-tandem mass spectrometry (HPLC-MS/MS)

analysis as described previously with modifications.²⁶ E2, 2E2 and 4E2 were separated on an Agilent Zorbax Bonus-RP column (2.1×150 mm, 5 µm). HPLC mobile phases consist of (A) water containing 0.1% formic acid and (B) acetonitrile containing 0.1% formic acid. After 1.0-min initial hold at 50% B, HPLC gradient increased to 70% B in 1 min and 95% in 0.05 min and remained at 95% B for 1.5 min before re-equilibration at 50% B. Flow rate was constant at 0.5 mL/min. The characteristic multiple reaction monitoring (MRM) transitions were 255.17→144.08 (positive ions for E2) and 287.24→161.23 (negative ions for 2E2 and 4E2). E2, 2E2 and 4E2 eluted at 2.7, 2.0 and 2.2 min, respectively. Metabolite identities were confirmed by comparing retention times to those of synthetic standards.

Targeted quantitative proteomic method for protein quantification

KLE cells (10-cm cell culture dish) were resuspended in a fractionation buffer (300 µl) containing 250 mM sucrose, 10 mM HEPES, 10 mM KCl, 1 mM EDTA, 1.5 mM MgCl₂, 1 mM dithiothreitol and protease inhibitor cocktail (cOmplete™, EDTA-free; Roche, Mannheim, Germany). Total cell lysates were obtained by passing the cell suspension 10 times through a 27-gauge needle, resting 10 min on ice, followed by another 10 passes. The resulting cell lysates were subjected to stepwise differential centrifugation to prepare microsomes: 10 min at 9,000×*g* and 60 min at 150,000×*g*, prior to resuspension of the final pellet in the fractionation buffer without the protease inhibitor cocktail. Microsomal protein content was determined using a BCA Protein Assay kit (Pierce).

Targeted proteomic quantification of CYP1B1, CYP1A1 and CYP1A2 protein levels in microsomal fractions was performed as described previously for other CYP enzymes with minor modifications.^{27, 28} Briefly, protein samples (30 µg) were reduced in an ammonium bicarbonate buffer (pH 8.0; 50 mM final concentration) containing dithiothreitol (4 mM final concentration) and heated at 60°C for 60 min to denature the proteins. After cooling to room temperature, the samples (90 µl total volume) were alkylated with iodoacetamide (10 mM final concentration) for 20 min in the dark and then digested with 1 µg trypsin at 37°C for 4 h. Recombinant human CYP1A1, CYP1A2 and CYP1B1 Supersomes of known concentrations (Corning Gentest, Woburn, MA) were used to create calibration standards (ranged from 0.002 to 5 pmol/digestion). All reactions were carried out in Protein LoBind microcentrifuge tubes (Eppendorf, Hamburg, Germany) to minimize protein or peptide loss due to binding. Reactions were quenched with storage at -80°C. The signature peptide sequences used were ELVALLVR for CYP1B1, GFYIPK for CYP1A1, and YLPNPALQR for CYP1A2. A mixture of stable isotope-labeled signature peptides (1 µl; Thermo Scientific, Ulm, Germany) were spiked into thawed samples as internal standards prior to loading onto an autosampler (6°C) for ultra-high pressure liquid chromatography-tandem mass spectrometry (UPLC-MS/MS) analysis as described previously.^{27, 28} Multiple reaction monitoring (MRM) transitions during UPLC-MS/MS analysis were *m/z* 456.8→571.4 for ELVALLVR, *m/z* 362.7→357.3 for GFYIPK, and *m/z* 536.6→584.4 for YLPNPALQR. The lower limit of quantification was 0.07 pmol CYP1B1, CYP1A1 or CYP1A2 per mg microsomal protein.

Cytotoxicity assay

Cytotoxicity was measured with a resazurin assay. Briefly, cells were seeded at 5,000 cells per well in a 96-well plate and maintained in a 5% CO₂ incubator at 37°C for 7 days for KLE and 24 h for HEK293T cells. Transfected HEK293T cells were treated with a probe prodrug at 48 h post-transfection. Drug treatment was initiated by adding prodrug-containing culture medium (0 – 100 μM; 100 μl/well) in the absence or presence of α-NF (10 μM). Treatment medium was changed every day. After a 69 h incubation with drug, cytotoxicity was determined by adding 20 μl of resazurin reagent (0.01% (w/v) resazurin sodium salt in phenol red-free DMEM) per well for an additional 3-h incubation (a total of 72 h incubation with drug). Fluorescence intensity was measured at 565 nm (excitation) and 595 nm (emission) using an Infinite[®] 200 PRO multimode reader. IC₅₀ values (drug concentration resulting in 50% cell death) were determined using the variable slope inhibitory dose-response curve (Prism 5.0; GraphPad Software, San Diego, CA). Vehicle (0.1% [v/v] DMSO) and Triton X-100 (2% [v/v]) were used as negative and positive controls, respectively.

Cell cycle analysis

The effect of probe prodrugs on KLE cell cycle was analyzed using a propidium iodide (PI) staining assay according to the manufacturer's protocol. Briefly, on day 7 post-seeding into 6-well tissue culture plates, KLE cells were treated with 10 or 100 μM prodrug in the absence or presence of α-NF (10 μM) for 72 h. Untreated cells were incubated without prodrug. Cells were harvested and fixed with 70% (v/v) ethanol and kept at –20°C overnight. PI staining was done at room temperature for 30 min before flow cytometry analysis (Beckman Coulter MoFlo[™] XDP FACS, Brea, CA). Data were analyzed using FlowJo software (version X.0.7; FLOWJO, LLC, Ashland, OR).

Apoptosis assay

The induction of apoptosis in KLE cells by probe prodrugs was analyzed using an Annexin V-FITC Apoptosis Detection kit according to the manufacturer's protocol. In all experiments, KLE cells were seeded in 6-well tissue culture plates and used day 7 post-seeding. In the first experiment, cells were treated with 50 μM DB289 or DB844 in the absence of α-NF for 24, 48 and 72 h. In the second experiment, cells were treated with 10, 50 and 100 μM DB289 or DB844 in the absence of α-NF for 72 h. Lastly, cells were treated with 50 μM DB289 or DB844 in the presence of α-NF (10 μM) for 24, 48 and 72 h. Untreated cells were incubated without prodrug. After the incubation, cells were collected and double stained with Annexin V and PI before flow cytometry analysis. Data were analyzed to determine viable, early apoptotic, and late apoptotic/necrotic cell populations.

Statistical analysis

All experiments were conducted in triplicate or quadruplicate, unless noted otherwise. Student's *t* tests (two-tailed, unpaired) were used to compare pairs of measurements (*e.g.*, effect of phenol red, effect of prodrugs on KLE and KLE-null cells, and effect of α-NF on pro-apoptotic effect of prodrugs in KLE cells). One-way analysis of variance (ANOVA) was used to compare multiple groups of measurements (*e.g.*, pro-apoptotic effect of prodrugs at

various conditions and effect of prodrugs on KLE cell cycle). All statistical analyses were performed using Prism 5.0 and $P < 0.05$ was considered significant.

RESULTS

Effect of culture conditions on *CYP1B1*, *CYP1A1* and *CYP1A2* expression in KLE cells

Since phenol red can have weak estrogenic activity²⁹ and *CYP1B1* and *CYP1A1* are regulated in part by the estrogen receptor^{30, 31}, it is necessary to determine the effect of phenol red on *CYP1* expression in KLE cells. Hence, *CYP1B1*, *CYP1A1* and *CYP1A2* expression in KLE cells were evaluated at different days post-seeding in the absence and presence of phenol red (Figure 1). Phenol red had little effect on *CYP1B1* expression (Figure 1A). In contrast, it markedly induced *CYP1A1* expression (Figure 1B) and had variable effects on *CYP1A2* expression (Figure 1C). Despite the marked induction of *CYP1A1* mRNA expression, EROD activity in KLE cells remained largely unchanged or slightly decreased due to the presence of phenol red (Figure 1D). Since *CYP1A1* is known to catalyze the EROD reaction, this suggests that induced *CYP1A1* mRNA expression was either not translated to protein expression or not to a level significant enough to alter the overall EROD activity in KLE cells. In addition, *CYP1B1* expression steadily increased from day 5 to day 9 post-seeding and remained relatively high through day 13 post-seeding (Figure 1A). EROD activity generally tracked with *CYP1B1* expression with a 1–2 day lag time, likely due to a delay in protein production relative to gene transcription. Based on these findings, KLE cells were cultured in phenol red-free medium in subsequent experiments to avoid *CYP1A1* induction and EROD inhibition. In addition, KLE cells from day 7 post-seeding were used in subsequent experiments when higher *CYP1B1* expression and function were desired.

CYP1B1 gene and protein expression in transiently transfected HEK293T cells

CYP1B1 gene expression reached the highest level at 24 h post-transfection in transiently transfected HEK293T cells (Figure 1E). However, it diminished quickly afterwards to 25% on day 2, 6% on day 5, and 2% on day 8. *CYP1B1* protein also was highest at 24 h post-transfection (1.5 pmol/mg microsomes) and decreased to 65% on day 2 and 42% on day 3 (Figure 1F). It was below the limit of detection (0.07 pmol/mg microsomes) in samples from empty vector controls and day 5 and day 8 post-transfection.

Comparison of *CYP1B1*, *CYP1A1* and *CYP1A2* expression in human liver, differentiated HepaRG, KLE and transfected HEK293T cells

CYP1B1 expression was highest in transiently transfected HEK293T cells 24 h post-transfection, followed by KLE cells at day 9 post-seeding (Figure 2A). Substantially lower levels of *CYP1B1* were found in differentiated HepaRG cells and human liver. In contrast, *CYP1A1* and *CYP1A2* expressions were lowest in KLE cells, but highest in differentiated HepaRG cells and human liver, respectively.

CYP1B1 protein expression and activity in KLE cells

CYP1B1 protein expression increased from day 3 to day 9 post-seeding (0.31 vs. 0.68 pmol/mg microsomes) and remained high on day 14 post-seeding (0.41 pmol/mg

microsomes) (Figure 2B). In contrast, CYP1A1 and CYP1A2 were not detected at the protein level in all KLE cell samples. Furthermore, CYP1B1-specific 4E2 formation was detected in KLE cells (Figure 2C).

Inhibition of CYP1B1 activity in KLE cells by α -NF

α -NF is a potent noncompetitive inhibitor ($K_i = 2.8$ nM) of CYP1B1 catalytic activity,³² but also potently inhibits CYP1A1 and CYP1A2. Here, we used it to inhibit the CYP1B1 activity of KLE cells in order to create CYP1B1-inhibited KLE cells. α -NF (1 μ M) inhibited the EROD activity of KLE cells by 81% over a 24 h incubation as measured by the area under the EROD fluorescence-incubation time curves (Figure 3A). In addition, α -NF, up to 15 μ M, did not show any cytotoxic effect on KLE cells (Figure 3B).

Differential cytotoxicity of CYP1B1-targeted probe prodrugs in KLE cells and CYP1B1-inhibited KLE cells

Two probe prodrugs DB289 and DB844 were used in this study to validate the KLE cell-based model for screening CYP1B1-targeted anticancer prodrugs. Both probe prodrugs (50 μ M) were more toxic to KLE cells than to CYP1B1-inhibited KLE cells (21% vs. 62% viability for DB289 and 16% vs. 44% viability for DB844) (Figures 4C and 4D). Furthermore, cytotoxicities (IC_{50} s) of DB289 and DB844 were determined for KLE cells, CYP1B1-transfected HEK293T cells, wild-type HEK293T cells and HepaRG cells in the absence or presence of 10 μ M α -NF (Table 1). Results showed that only KLE cells demonstrated a moderate difference (1.2 to 1.5-fold) in IC_{50} values in response to CYP1B1 inhibition by α -NF.

Effect of probe prodrugs on cell cycle in KLE cells and CYP1B1-inhibited KLE cells

To determine if alterations in cell cycle contributed to the differential cytotoxicities of the probe prodrugs towards KLE cells and CYP1B1-inhibited KLE cells, cell cycle analysis was performed on cells treated with DB289 or DB844 (10 and 100 μ M) for 72 h. Percent cell populations in various stages of cell cycle were summarized in Table 2. Both DB289 and DB844 induced a concentration-dependent G0/G1 cell cycle arrest in KLE cells, as well as a reduction in the S phase population, compared to untreated cells. However, these cell cycle effects were absent in CYP1B1-inhibited KLE cells, suggesting a requirement for CYP1B1 activity.

Pro-apoptotic effect of probe prodrugs in KLE cells and CYP1B1-inhibited KLE cells

Both DB289 and DB844 exhibited a similar pro-apoptotic effect on KLE cells at different treatment times as determined by a significant increase in the early apoptotic cell population relative to untreated cells (Figure 4A). In addition, both probe prodrugs exhibited concentration-dependent pro-apoptotic effects in KLE cells (Figure 4B). Furthermore, these pro-apoptotic effects were compared between KLE cells and CYP1B1-inhibited KLE cells. Results showed that addition of α -NF (10 μ M) attenuated the pro-apoptotic effect of both probe prodrugs as evidenced by a significant reduction of the early apoptotic cell population between KLE cells and CYP1B1-inhibited KLE cells, although the effect was more evident with DB844 than DB289 (Figures 5C and 5D).

DISCUSSION

The primary objective of the current study was to develop KLE cell line as a relevant drug discovery model for screening CYP1B1-targeted anticancer prodrugs. Several lines of evidence supported the use of a KLE cell-based screening model for this purpose. First, KLE cells alone expressed appreciable levels of CYP1B1, which remained relatively stable to at least two weeks post-seeding (Figure 1). Formation of 4E2 from E2 was detected in KLE cells (Figure 2C), which was a reaction specifically catalyzed by CYP1B1.³ KLE cells also were superior to transiently-transfected HEK293T cells as CYP1B1 expression quickly diminished in the transfected cells. This quickly diminished expression likely contributed to the lack of difference in prodrug cytotoxicity in the absence or presence of α -NF in CYP1B1-HEK293T cells (Table 1). Second, two probe prodrugs, DB289 and DB844, showed differential cytotoxicities towards KLE cells and CYP1B1-inhibited KLE cells (Figures 4C, 4D and Table 1). Cell cycle and apoptosis analyses confirmed that CYP1B1 played an important role in mediating these effects in KLE cells (Table 2, Figures 5C and 5D). Third, the KLE cell line was derived from a poorly differentiated endometrial carcinoma and possesses tumorigenic activity in nude mice.²³ This would make it possible to use the same cell line for generating a xenograft tumor model in mice in order to evaluate the *in vivo* efficacy of potential CYP1B1-targeted anticancer prodrugs. As such, we propose a new screening model that consists of KLE cells and CYP1B1-inhibited KLE cells, achieved with α -NF treatment, to identify molecules that exhibit preferential cytotoxicity in KLE cells and not CYP1B1-inhibited KLE cells.

Although the two probe prodrugs DB289 and DB844 exhibited preferential cytotoxicity to KLE cells, they lack anticancer potency due to weak cytotoxicity (low-to-mid micromolar IC₅₀s) and a small, albeit significant, difference in relative cytotoxicity (1.2 to 1.5-fold; Table 1). Since the maximal plasma concentration of DB289 was below 1 μ M after a single oral dose of 100 mg in healthy human volunteers (maximally tolerated dose for a twice daily regimen),³³ it is impossible to further develop DB289 as a CYP1B1-targeted anticancer prodrug. The same is true for DB844, as it only reached an average maximal plasma concentration of 0.43 μ M after the 14th daily oral administration of the maximally tolerated dose (6 mg/kg) in vervet monkeys.³⁴

To discover new CYP1B1-targeted anticancer prodrugs, screening of large chemical libraries using the proposed screening model should be further developed and conducted. However, it is still unclear what selection criteria should be set for screening. DB289 and DB844 only achieved a minimal difference in cytotoxicity (*i.e.*, IC₅₀ ratio) against KLE cells and CYP1B1-inhibited KLE cells. In theory, a much greater IC₅₀ ratio would be preferred in order to enhance prodrug targeting against CYP1B1-expressing tumor tissues, while protecting normal tissues from the harmful effect of active metabolites. Moreover, in addition to using KLE cells and CYP1B1-inhibited KLE cells for primary screening, counter screens should be implemented to eliminate candidate prodrugs that also are activated by other P450 enzymes (*e.g.*, CYP1A2 and CYP3A4). Such counter screens could be established using primary human hepatocytes, transfected cell lines or a panel of recombinant CYP enzymes.^{22, 35}

In summary, KLE cells have been shown to exclusively express appreciable levels of CYP1B1. Additionally, a KLE cell-based screening model has been characterized using two probe prodrugs and thus proposed as a relevant drug discovery model that can be potentially developed to screen chemical libraries to discover novel CYP1B1-targeted anticancer prodrugs.

Supplementary Material

Refer to Web version on PubMed Central for supplementary material.

ACKNOWLEDGEMENT

This work was supported in part by the United States National Institutes of Health [R01GM089994].

Nonstandard abbreviations:

CYP	cytochrome P450
DMSO	dimethyl sulfoxide
E2	17 β -estradiol
2E2	2-hydroxylated 17 β -estradiol
4E2	4-hydroxylated 17 β -estradiol
7-ER	7-ethyl-resorufin
EROD	ethoxyresorufin-O-deethylase
IC₅₀	concentration of inhibitor at 50% maximal inhibition
MRM	multiple reaction monitoring
MTBE	methyl tert-butyl ether
α-NF	α -naphthoflavone
UPLC-MS/MS	ultra-high pressure liquid chromatography-tandem mass spectrometry

REFERENCES

1. Ortiz de Montellano PR Cytochrome P450 - Structure, Mechanism, and Biochemistry (4th Edition). Springer International Publishing: 2015; p 912.
2. Shimada T; Hayes CL; Yamazaki H, et al. Activation of chemically diverse procarcinogens by human cytochrome P-450 1B1. *Cancer Res* 1996, 56 (13), 2979–84. [PubMed: 8674051]
3. Hayes CL; Spink DC; Spink BC, et al. 17 beta-estradiol hydroxylation catalyzed by human cytochrome P450 1B1. *Proc Natl Acad Sci U S A* 1996, 93 (18), 9776–81. [PubMed: 8790407]
4. McKay JA; Melvin WT; Ah-See AK, et al. Expression of cytochrome P450 CYP1B1 in breast cancer. *FEBS Lett* 1995, 374 (2), 270–2. [PubMed: 7589551]

5. Gibson P; Gill JH; Khan PA, et al. Cytochrome P450 1B1 (CYP1B1) is overexpressed in human colon adenocarcinomas relative to normal colon: implications for drug development. *Mol Cancer Ther* 2003, 2 (6), 527–34. [PubMed: 12813131]
6. Tokizane T; Shiina H; Igawa M, et al. Cytochrome P450 1B1 is overexpressed and regulated by hypomethylation in prostate cancer. *Clin Cancer Res* 2005, 11 (16), 5793–801. [PubMed: 16115918]
7. Saini S; Hirata H; Majid S, et al. Functional significance of cytochrome P450 1B1 in endometrial carcinogenesis. *Cancer Res* 2009, 69 (17), 7038–45. [PubMed: 19690133]
8. McFadyen MC; Cruickshank ME; Miller ID, et al. Cytochrome P450 CYP1B1 over-expression in primary and metastatic ovarian cancer. *Br J Cancer* 2001, 85 (2), 242–6. [PubMed: 11461084]
9. Liu JY; Yang Y; Liu ZZ, et al. Association between the CYP1B1 polymorphisms and risk of cancer: a meta-analysis. *Mol Genet Genomics* 2015, 290 (2), 739–65. [PubMed: 25475389]
10. Li C; Long B; Qin X, et al. Cytochrome P1B1 (CYP1B1) polymorphisms and cancer risk: a meta-analysis of 52 studies. *Toxicology* 2015, 327, 77–86. [PubMed: 25434509]
11. Zhang H; Li L; Xu Y CYP1B1 polymorphisms and susceptibility to prostate cancer: a meta-analysis. *PLoS one* 2013, 8 (7), e68634. [PubMed: 23861929]
12. Gajjar K; Martin-Hirsch PL; Martin FL CYP1B1 and hormone-induced cancer. *Cancer Lett* 2012, 324 (1), 13–30. [PubMed: 22561558]
13. McFadyen MC; Murray GI Cytochrome P450 1B1: a novel anticancer therapeutic target. *Future Oncol* 2005, 1 (2), 259–63. [PubMed: 16555997]
14. Guengerich PF; Chun YJ; Kim D, et al. Cytochrome P450 1B1: a target for inhibition in anticarcinogenesis strategies. *Mutat Res* 2003, 523–524, 173–82.
15. Spink DC; Eugster HP; Lincoln DW 2nd, et al. 17 beta-estradiol hydroxylation catalyzed by human cytochrome P450 1A1: a comparison of the activities induced by 2,3,7,8-tetrachlorodibenzo-p-dioxin in MCF-7 cells with those from heterologous expression of the cDNA. *Arch Biochem Biophys* 1992, 293 (2), 342–8. [PubMed: 1536570]
16. Liehr JG; Fang WF; Sirbasku DA, et al. Carcinogenicity of catechol estrogens in Syrian hamsters. *Journal of steroid biochemistry* 1986, 24 (1), 353–6. [PubMed: 3009986]
17. Liehr JG; Ricci MJ 4-Hydroxylation of estrogens as marker of human mammary tumors. *Proc Natl Acad Sci U S A* 1996, 93 (8), 3294–6. [PubMed: 8622931]
18. Liehr JG; Ricci MJ; Jefcoate CR, et al. 4-Hydroxylation of estradiol by human uterine myometrium and myoma microsomes: implications for the mechanism of uterine tumorigenesis. *Proc Natl Acad Sci U S A* 1995, 92 (20), 9220–4. [PubMed: 7568105]
19. Shatalova EG; Klein-Szanto AJ; Devarajan K, et al. Estrogen and cytochrome P450 1B1 contribute to both early- and late-stage head and neck carcinogenesis. *Cancer Prev Res (Phila)* 2011, 4 (1), 107–15. [PubMed: 21205741]
20. Sale S; Tunstall RG; Ruparelia KC, et al. Effects of the potential chemopreventive agent DMU-135 on adenoma development in the ApcMin+ mouse. *Invest New Drugs* 2006, 24 (6), 459–64. [PubMed: 16505954]
21. Potter GA; Patterson LH; Wanogho E, et al. The cancer preventative agent resveratrol is converted to the anticancer agent piceatannol by the cytochrome P450 enzyme CYP1B1. *Br J Cancer* 2002, 86 (5), 774–8. [PubMed: 11875742]
22. Vinader V; Sadiq M; Sutherland M, et al. Probing cytochrome P450-mediated activation with a truncated azinomycin analogue. *MedChemComm* 2015, 6 (1), 187–191.
23. Richardson GS; Dickersin GR; Atkins L, et al. KLE: a cell line with defective estrogen receptor derived from undifferentiated endometrial cancer. *Gynecol Oncol* 1984, 17 (2), 213–30. [PubMed: 6706226]
24. Wang MZ; Saulter JY; Usuki E, et al. CYP4F enzymes are the major enzymes in human liver microsomes that catalyze the O-demethylation of the antiparasitic prodrug DB289 [2,5-bis(4-amidinophenyl)furan-bis-O-methylamidoxime]. *Drug Metab Dispos* 2006, 34 (12), 1985–94. [PubMed: 16997912]
25. Ju W; Yang S; Ansede JH, et al. CYP1A1 and CYP1B1-mediated biotransformation of the antitrypanosomal methamidoxime prodrug DB844 forms novel metabolites through intramolecular rearrangement. *Journal of pharmaceutical sciences* 2014, 103 (1), 337–49. [PubMed: 24186380]

26. Keski-Rahkonen P; Huhtinen K; Poutanen M, et al. Fast and sensitive liquid chromatography-mass spectrometry assay for seven androgenic and progestagenic steroids in human serum. *J Steroid Biochem Mol Biol* 2011, 127 (3–5), 396–404. [PubMed: 21684334]
27. Michaels S; Wang MZ The revised human liver cytochrome P450 “Pie”: absolute protein quantification of CYP4F and CYP3A enzymes using targeted quantitative proteomics. *Drug Metab Dispos* 2014, 42 (8), 1241–51. [PubMed: 24816681]
28. Wang MZ; Wu JQ; Dennison JB, et al. A gel-free MS-based quantitative proteomic approach accurately measures cytochrome P450 protein concentrations in human liver microsomes. *Proteomics* 2008, 8 (20), 4186–96. [PubMed: 18792928]
29. Berthois Y; Katzenellenbogen JA; Katzenellenbogen BS Phenol red in tissue culture media is a weak estrogen: implications concerning the study of estrogen-responsive cells in culture. *Proc Natl Acad Sci U S A* 1986, 83 (8), 2496–500. [PubMed: 3458212]
30. Tsuchiya Y; Nakajima M; Kyo S, et al. Human CYP1B1 is regulated by estradiol via estrogen receptor. *Cancer Res* 2004, 64 (9), 3119–25. [PubMed: 15126349]
31. Angus WG; Larsen MC; Jefcoate CR Expression of CYP1A1 and CYP1B1 depends on cell-specific factors in human breast cancer cell lines: role of estrogen receptor status. *Carcinogenesis* 1999, 20 (6), 947–55. [PubMed: 10357772]
32. Rochat B; Morsman JM; Murray GI, et al. Human CYP1B1 and anticancer agent metabolism: mechanism for tumor-specific drug inactivation? *J Pharmacol Exp Ther* 2001, 296 (2), 537–41. [PubMed: 11160641]
33. Yan GZ; Generaux CN; Yoon M, et al. A semiphysiologically based pharmacokinetic modeling approach to predict the dose-exposure relationship of an antiparasitic prodrug/active metabolite pair. *Drug Metab Dispos* 2012, 40 (1), 6–17. [PubMed: 21953913]
34. Thuita JK; Wang MZ; Kagira JM, et al. Pharmacology of DB844, an orally active aza analogue of pafuramidine, in a monkey model of second stage human African trypanosomiasis. *PLoS neglected tropical diseases* 2012, 6 (7), e1734. [PubMed: 22848769]
35. Sheldrake HM; Travica S; Johansson I, et al. Re-engineering of the duocarmycin structural architecture enables bioprecursor development targeting CYP1A1 and CYP2W1 for biological activity. *J Med Chem* 2013, 56 (15), 6273–7. [PubMed: 23844629]

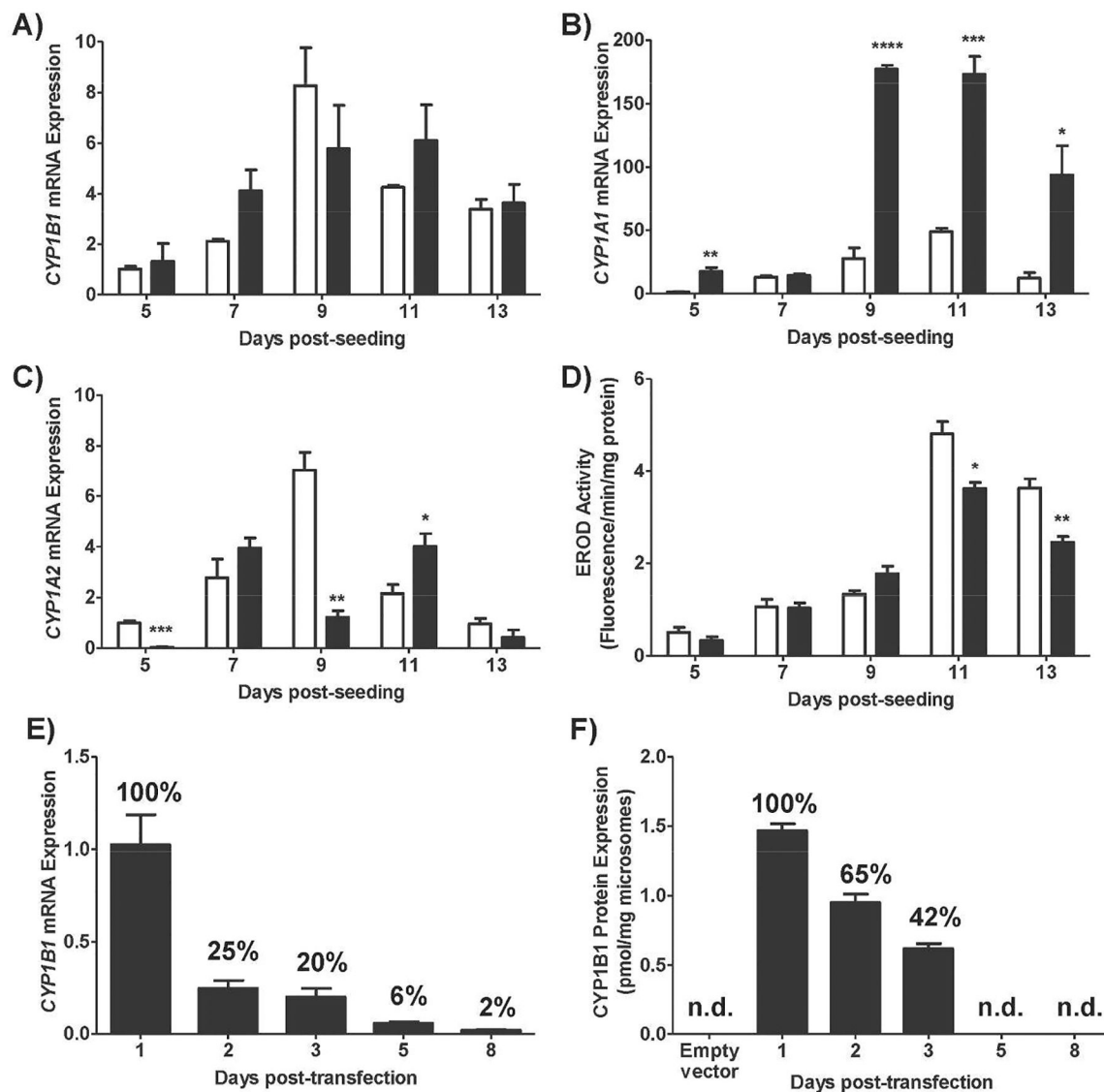


Figure 1. Effect of phenol red and culture time on gene expression of (A) *CYP1B1*, (B) *CYP1A1* and (C) *CYP1A2*, and on (D) EROD activity in KLE cells and effect of culture time on *CYP1B1* (E) gene and (F) protein expression after transient transfection in HEK293T cells.

For KLE cells, gene expression and EROD activity were determined at different days post-seeding in the absence (open bars) and presence (filled bars) of phenol red. Gene expression was normalized to samples from day 5 post-seeding without phenol red. For HEK293T cells, *CYP1B1* protein concentrations were determined using the targeted quantitative proteomic method described in Materials and Methods. Bars and error bars represent the mean and standard error of triplicate determinations. Student's *t* test (two-tailed) was used to compare the effect of phenol red (*, $P < 0.05$; **, $P < 0.01$; ***, $P < 0.001$; ****, $P < 0.0001$). n.d., not detected.

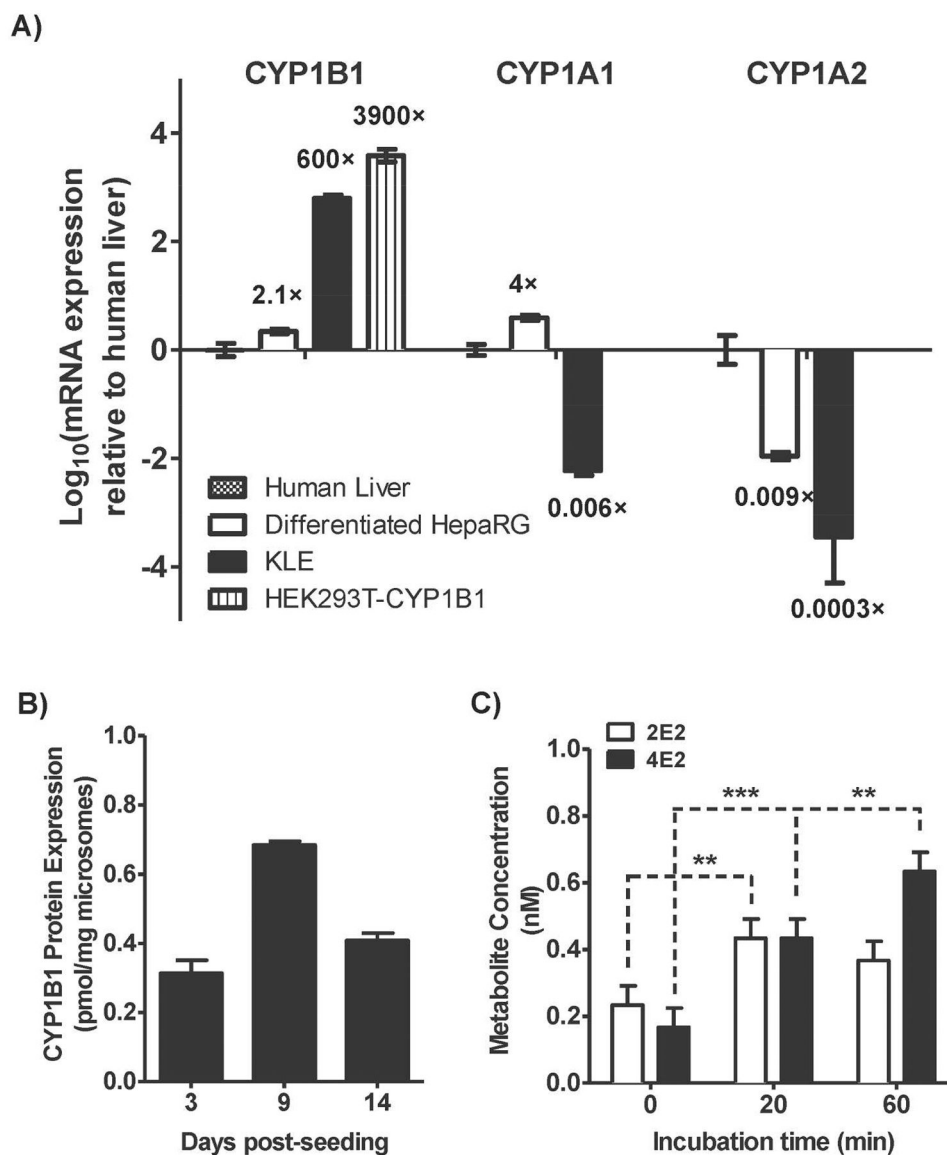


Figure 2. Relative gene expression (A) of *CYP1B1*, *CYP1A1* and *CYP1A2* in human liver, differentiated HepaRG cells, KLE cells and HEK293T cells transiently transfected with *CYP1B1* and CYP1B1 protein expression (B) and activity (C) in KLE cells.

Human liver total RNA (catalog # 540017; pool of 3 donors) was purchased from Agilent Technologies. Differentiated HepaRG cells were prepared after 2-week incubation in Differentiation medium. KLE cells were prepared 9 days post-seeding. Transfected HEK293T cells were prepared 24 h post-transfection. CYP1B1 protein concentrations and activity (4E2 formation from E2) were determined using the targeted quantitative proteomic method and the E2 hydroxylation assay described in Materials and Methods. Bars and error bars represent the mean and standard deviation of triplicate determinations. One-way ANOVA with Dunnett post test (**, $P < 0.01$; ***, $P < 0.001$) was used to compare metabolite formation at 20 and 60 min to the control at 0 min.

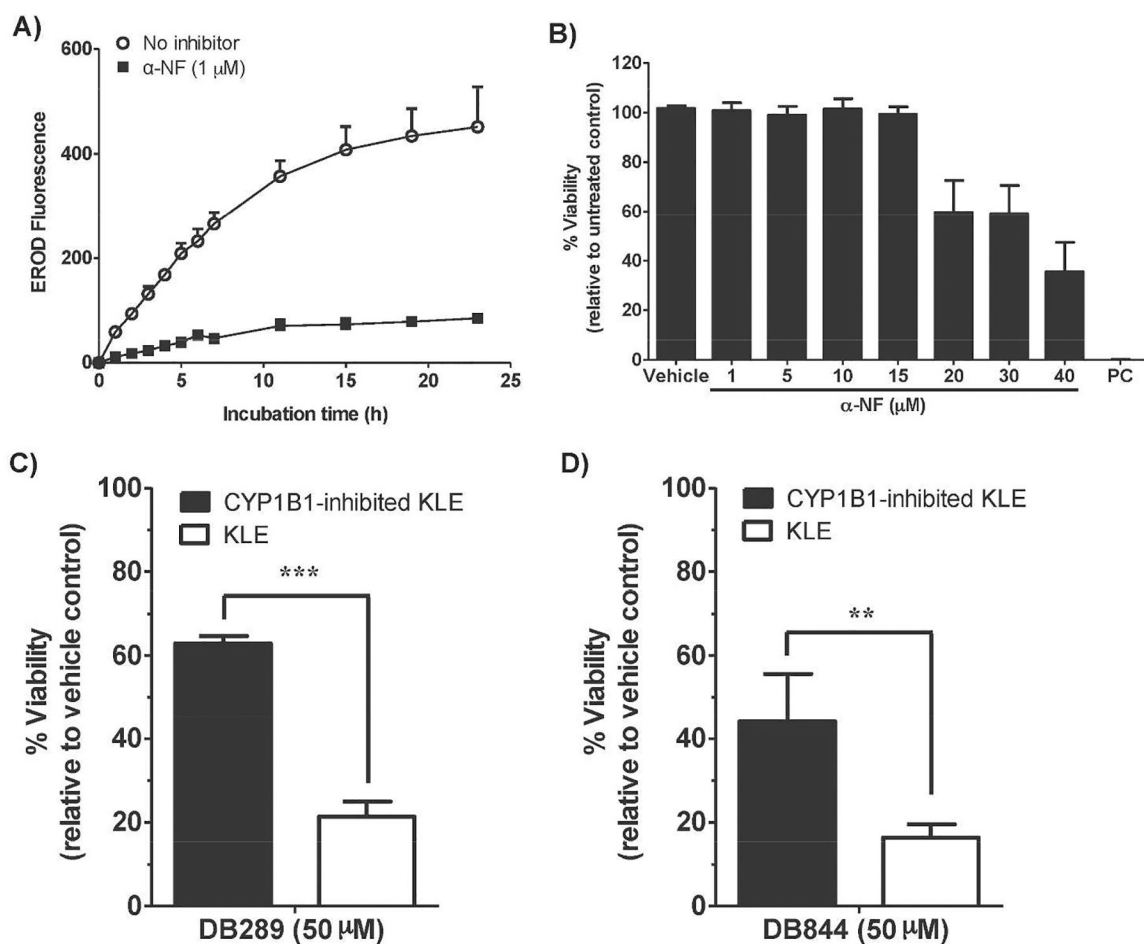


Figure 3. Inhibitory (A) and cytotoxic effects (B) of the CYP1B1 inhibitor α -NF in KLE cells and differential cytotoxicity of probe prodrugs DB289 (C) and DB844 (D) on KLE cells and CYP1B1-inhibited KLE cells.

CYP1B1 activity in KLE cells was determined using the EROD assay. Viability of KLE cells under different treatments was normalized to untreated vehicle control. The positive control (PC) contained 2% (v/v) Triton X-100. Symbols (or bars) and error bars represent the mean and standard deviation of triplicate determinations (A and B) or quadruplicate determinations (C and D). Student's *t* test (two-tailed) was used to compare the effect of CYP1B1 inhibitor α -NF (**, P 0.01; ***, P 0.001).

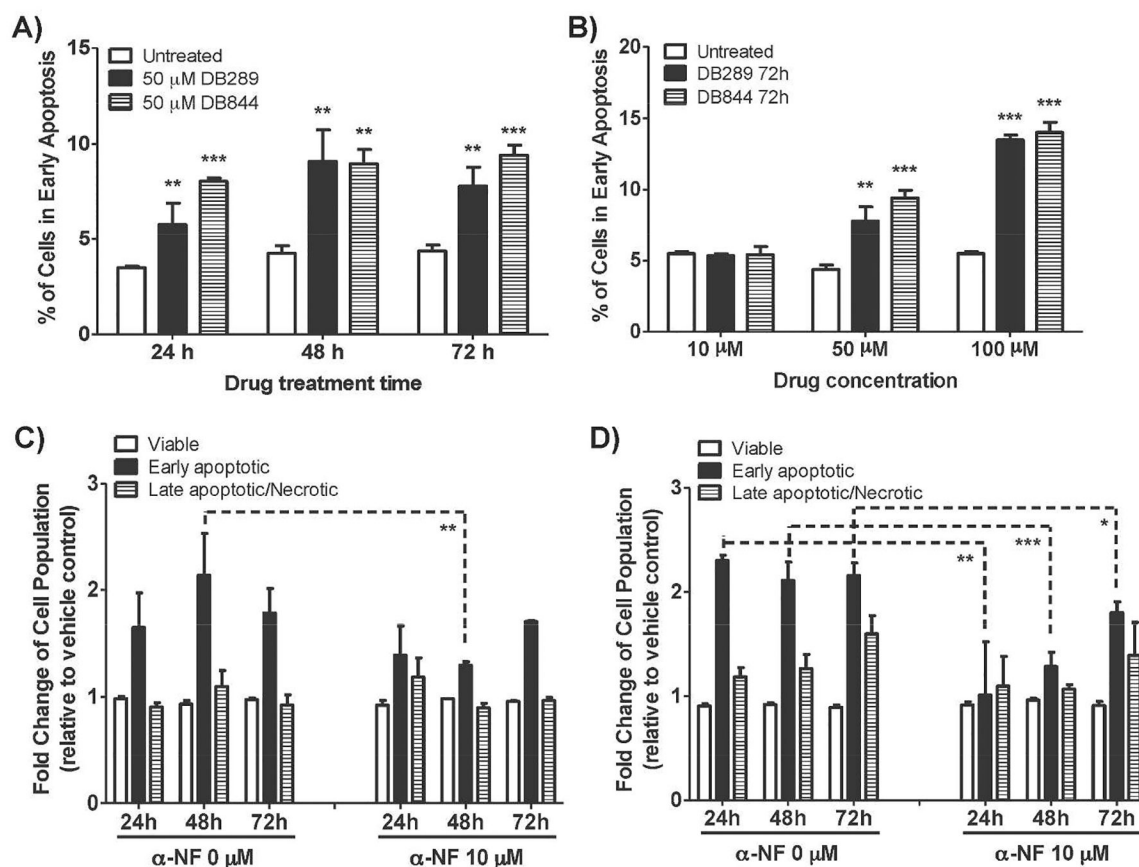


Figure 4. Pro-apoptotic effects of probe prodrugs DB289 and DB844 on KLE cells in the absence and presence of a CYP1B1 inhibitor α -NF.

In the absence of α -NF, percentage of cells in early apoptosis was compared (A) between different treatments to untreated controls at various lengths of treatment time and (B) between different treatments to untreated controls at various drug concentrations after 72 h incubation using one-way ANOVA with Dunnett post test (**, P 0.01; ***, P 0.001). Then, effect of α -NF on the pro-apoptotic effect of probe prodrugs (C) DB289 and (D) DB844 in KLE cells was evaluated by comparing the fold-change in the percentage of cell populations (viable, early apoptotic and late apoptotic/necrotic) between without and with α -NF (10 μ M) treatment at different lengths of incubation time (24, 48, and 72 h) using two-tailed Student's t test (*, P 0.05; **, P 0.01; ***, P 0.001). Bars and error bars represent the mean and standard deviation of triplicate determinations.

Table 1.Differential cytotoxicity (IC₅₀) of probe prodrugs DB289 and DB844.

Treatment		KLE	CYP1B1-HEK293T	HEK293T	HepaRG
Prodrug	α -NF ^a				
DB289	-	54.9 ± 1.0 ^b	57.6 ± 1.6	57.9 ± 5.4	82.5 ± 1.4
	+	84.1 ± 2.1	61.8 ± 1.6	57.4 ± 6.1	87.6 ± 2.4
DB844	-	57.9 ± 1.3	38.8 ± 0.9	37.9 ± 0.9	76.3 ± 1.6
	+	72.1 ± 1.2	37.5 ± 0.6	38.9 ± 0.9	82.2 ± 2.2

^a α -NF concentration was 10 μ M.^bValues are IC₅₀ ± standard errors after nonlinear regression analysis of quadruplicate determinations at individual concentration.

Author Manuscript

Author Manuscript

Author Manuscript

Author Manuscript

Table 2.

Cell cycle analysis of KLE cells treated with probe prodrugs DB289 and DB844.

Prodrug	Treatment		Sub-G1	G0/G1	S	G2/M	>4N
	α -NF ^b						
Untreated	-		5.2 ± 1.0 ^b	36.8 ± 3.5	13.6 ± 0.1	44.7 ± 0.5	3.4 ± 0.7
DB289	10 μ M	-	5.1 ± 1.4	40.0 ± 1.7	5.3 ± 1.1 ^{***}	45.0 ± 5.2	1.7 ± 0.6
	100 μ M	-	4.5 ± 0.7	43.2 ± 0.8 [*]	8.3 ± 1.0 ^{***}	39.5 ± 0.2	4.5 ± 1.3
DB844	10 μ M	-	4.6 ± 0.8	38.7 ± 2.1	8.0 ± 1.4 ^{***}	47.3 ± 0.5	6.3 ± 1.9
	100 μ M	-	5.3 ± 1.5	43.9 ± 1.2 ^{**}	6.6 ± 1.1 ^{**}	40.6 ± 1.3	3.7 ± 0.9
Untreated	+		5.2 ± 1.6	42.0 ± 4.0	9.0 ± 2.5	38.8 ± 5.8	3.9 ± 1.7
DB289	10 μ M	+	5.4 ± 0.0	39.5 ± 0.6	9.8 ± 1.4	39.3 ± 2.9	5.3 ± 1.0
	100 μ M	+	4.7 ± 1.0	43.2 ± 3.4	6.1 ± 1.1	42.4 ± 2.6	3.6 ± 0.4
DB844	10 μ M	+	4.1 ± 1.1	41.1 ± 1.5	7.9 ± 1.5	40.7 ± 2.9	4.9 ± 0.9
	100 μ M	+	4.3 ± 0.9	43.3 ± 0.4	5.6 ± 0.7	41.8 ± 1.1	3.4 ± 0.6

^aValues denote % of cells in each phase of cell cycle and represent means ± standard deviations of triplicate determinations.^b α -NF concentration was 10 μ M.^{*} $P < 0.05$,^{**} $P < 0.01$,^{***} $P < 0.0001$,compared to untreated cells of the corresponding α -NF treatment group (one-way ANOVA with Dunnett post test).